

Bonding Fixture Tolerances for High-Volume Metal Microlamination Based on Fin Buckling and Laminae Misalignment Behavior

Wassanai Wattanutchariya

Department of Industrial Engineering, Faculty of Engineering, Chiangmai University, Chiangmai 50200, Thailand
(011-6653) 944125, wattanwa@yahoo.com

Brian K. Paul

Department of Industrial and Manufacturing Engineering, Oregon State University, 118 Covell Hall, Corvallis, OR
97330 USA, 541-737-7320, fax: 541-737-5241, brian.paul@orst.edu

Abstract

Microlamination involves the patterning, registration and bonding of thin layers of material, called laminae, to produce monolithic devices with embedded micro-scale features. In energy, chemical and biological systems miniaturization, microlamination can be used to produce bulk microfluidic devices for mobile, compact or point-of-use applications. Thermally-Enhanced Edge Registration (TEER) is a registration technique used in metallic microlamination to precisely align laminae during high-temperature bonding cycles. Shape variation, such as channel misalignment or fin buckling, incurred during the TEER registration step can lead to lower system performance or even functional failure. This paper investigates the allowable tolerance limits in TEER fixtures in order to minimize fin buckling while attaining precise alignment. A high-temperature buckling model is developed to predict the onset of fin buckling within a TEER fixture. The results of the model are validated empirically. Results indicate that within the tolerance limits, μm -scale channel-to-channel alignment can be achieved free of fin buckling. In addition, the general relationship between the critical point of buckling and the device configuration is discussed for broader application.

Keywords: Microlamination; Bulk microfluidic devices; High temperature; Registration; Buckling theory; Fixture tolerances

Microtechnology-based Energy and Chemical Systems (MECS) are devices which process bulk fluids within highly-paralleled arrays of microchannels. These miniaturized energy and chemical systems enable large quantities of fluid to be processed without requisite pressure drop penalties. The use of microchannels results in shorter diffusional distances which permit shorter residence times in channels, shorter channel lengths and, ultimately, no increase in pressure drop. MECS devices have the potential to revolutionize the processing of mass and energy where a premium is placed on mobility, compactness, or point-of-use production. The miniaturization of bulk chemical and energy unit operations through the application of MECS devices is called process intensification (PI).

By and large, PI devices are produced through microlamination techniques involving the patterning, registration and bonding of thin material sheets or laminae. Microlamination techniques have been used to prototype a variety of PI devices for application in advanced climate control¹, solvent separation², microcombustion³, fuel processing⁴, high-temperature catalysis⁵ and fluidic control⁶ among others. Bulk microfluidic devices have been constructed in a wide array of materials with features as small as several μm . In addition to being used for PI, microlamination methods have been used in the past in applications ranging from pneumatic control systems to rocket engine fuel injection assemblies.^{7,8,9,10,11} Even so, the major commercial impact of these methods has been limited mainly to non-bulk fluid processing applications including inkjet printing and more recently lab-on-a-chip for the life sciences.^{12,13} Figure 1 shows the lamination scheme for fabricating a counterflow microchannel array, which could be used as a recuperative heat exchanger in PI applications.

Several previous investigations have found that the registration step is critical in microlamination. Paul, et al.¹⁴ found that poor registration in intermetallic microchannel devices resulted in an

amplification in the fin warpage found within the device. Ashley¹⁵ found that layer-to-layer bearing gaps on the order of 10 μm were necessary in order to operate the micro-scale turbine generator developed at MIT. In each of these applications, precision alignment of laminae was necessary in order to produce a functional device. Several registration techniques have been employed in microlamination methods including pin, edge, and self-alignment. The technique used depends on the bonding process chosen. The registration technique investigated in this study is called Thermally-Enhanced Edge Registration (TEER).¹⁶ This technique can be used to register laminae during the high temperature diffusion bonding of polycrystalline metals. The TEER technique employs the difference in CTE between the bonding fixture and the laminated material to produce a registration force on the laminae at the bonding temperature. By making the bonding fixture from a material that has a lower CTE than the laminae, a clearance will exist between the fixture and the laminae at room temperature, making the loading of laminae simple compared with other mechanical alignment methods. At the same time, TEER is able to achieve a layer-to-layer registration accuracy as small as 5 μm .

During diffusion bonding, the metal laminae and the bonding fixture are heated up to a specific temperature, normally in the range of about 60% to 75% of the melting temperature of the base material. For metallic structures, this temperature can be 1000 $^{\circ}\text{C}$ or higher. Within a TEER procedure, the fixture and laminae will expand differently as the temperature is raised resulting in a registration force on the laminae at the bonding temperature. However, if this registration force is higher than the critical buckling load of the microchannel fin, buckling of the fin will occur. This is illustrated in Figure 2. When buckling develops, flow channels that are separated by the buckled fin are no longer uniform resulting in flow maldistribution and a drop in effectiveness of the microchannel array.

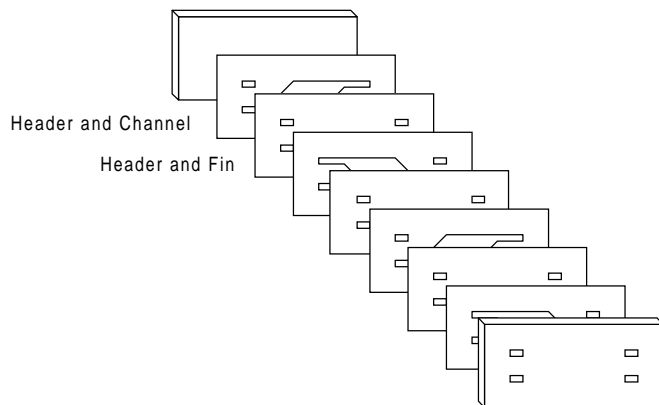


Figure 1. A schematic of microlamination procedure for producing a two-fluid counter-flow microchannel array



Figure 2. SEM micrographs of a microchannel heat exchanger with nonuniform flow channels after fin buckling

Figure 3 illustrates the result from a previous investigation conducted on TEER technique for stainless steel microlamination.¹⁷ The graph shows the relationship between the allowance of the bonding fixture and laminae versus the amount of misalignment. This picture suggests that there is an interval of allowance between the laminae and the bonding fixture, where the misalignment is somewhat constant. From this graph, it is observed that once interference is established the accuracy of registration is not improved further. On the other hand, if this interference extends beyond a certain point, the fin will buckle. This indicates that interference should remain within a particular range. This range should constrain the allowable tolerance of the fixture, governed by the desired registration accuracy and the buckling of the laminae. The goal for this study is to predict the tolerance limits of TEER fixtures based on buckling theory and registration behavior.

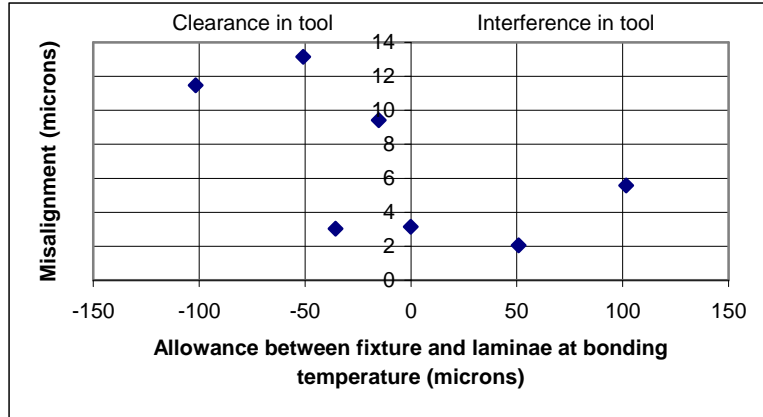


Figure 3. Graph of misalignment versus allowance between fixture and laminae at bonding temperature

To determine if a fin will buckle, the mode of failure needs to be confirmed by calculating several loads. For the fixed-ended boundary condition, the critical buckling load (P_c) can be calculated from:

$$P_c = \frac{4 * \pi^2 * E * I}{L_s^2} \quad (1)$$

where L_s is the fixture slot width at room temperature, E is Young's Modulus and I is the moment of inertia of the specimen. The second load to be considered is the yield load (P_y) defined as the load necessary to yield the fin in compression which is the product of the yield strength and the cross sectional area of the fin:

$$P_y = \sigma_p \cdot A_f \quad (2)$$

The final load to be considered is called the registration load (P_r) due to thermal expansion which occurs beyond the temperature at which the dimension of the fixture and laminae are equal to each other (called the registration temperature). The registration load can be calculated from:

$$P_r = A_f * E * (\alpha_{ss} - \alpha_g) * \Delta T_{eff} \quad (3)$$

where, in this investigation, α_{ss} is the CTE of stainless steel and α_g is the CTE of graphite and ΔT_{eff} is the temperature increase beyond the registration temperature at which the onset of inelastic buckling occurs (i.e. the bonding temperature must be above the registration temperature in order to produce a load).

If the yield load is greater than the critical load for fin buckling, the fin may buckle elastically if the registration force is less than the yield force. However, in the case where the critical load for fin buckling is greater than the yield load, the fin may yield in compression without buckling if the registration load is larger than the yield load but below the critical load for fin buckling¹⁷. In either case, if the registration load exceeds both the critical load for fin buckling and the yield load, the fin will permanently buckle.

The test specimen used in this experiment consisted of two-channel layers and a fin layer. All layers were made from a 304 stainless steel shim. A Nd:YAG laser operating at the fourth harmonic was used to pattern the shims of three different thicknesses (0.0508 mm, 0.0762 mm and 0.1016 mm). After patterning, all laminae were polished and cleaned with an ultrasonic cleaner to remove slag resulted from the laser machining process. Then, the fin lamina was measured by a Dektak3 surface profiler to record the initial flatness characteristics. Before bonding, all laminae were rinsed with Acetone, Ethanol, and De-ionized water (AED) to remove grease or any other residues on the surfaces so that a sound diffusion-bonded joint could be formed.

The fixture assembly was then put in a vacuum hot press chamber, and the bonding cycle began. The first step in the bonding process involved pumping down the chamber to achieve a satisfactory vacuum (approximately 10^{-4} mbar). The system was then heated up to the appropriate bonding temperature. Once the bonding temperature was reached, clamping pressure was applied to the fixture to

induce the diffusion bond. At the end of the bonding phase, the clamping pressure was removed so that the laminate could contract uniformly without inducing residual stress. The bonding conditions for this experiment were set up at 750 °C with 5 MPa applied pressure and a one hour dwell period. After the system cooled down, the laminate was taken out to check for possible characteristics of fin deflection using the surface profiler. Similar to the initial flatness measurements, warpage measurements were also taken to record the post-bonding characterization. The average deflection and standard deviation of each sample were calculated and were used for theoretical comparisons.

The allowance between fin width and the fixture slot was varied in order to evaluate the relationship between the fixture allowance and both types of shape variation. Fins with thicknesses ranging from 0.0508 mm to 0.1016 mm were used in this study. In general, the critical point of buckling is proportional to the thickness of the fin layer. The thicker the material, the greater the strength and the greater amount of interference needed before the fin starts buckling. However, this critical buckling load also needs to exceed the proportional limit of yield strength (or elastic property) to cause the fin to be permanently deformed after bonding. For laminae with thicknesses below 0.1016 mm, the load at the proportional limit is found greater than the critical point of buckling; therefore, all specimens in this experiment should have the same buckling behavior.*

The first experimental set up was designed to evaluate the effect of fin thickness on the buckling behavior of the fin. Since the buckling behavior of all fins in this experiment was supposed to be the same, each thickness was only tried at each 2 allowances. The significance of the thickness was checked using an analysis of variance (ANOVA). An additional test was performed to evaluate the difference between the theoretical and the experimental results. A paired t-test was used to verify this comparison based on the null hypothesis that the mean of the difference in theoretical data and experimental results is zero with alpha equal to 0.05. If both theoretical and experimental results are equal, a 95% confidence interval for the mean difference must include zero.

The measurement of channel-to-channel misalignment was performed at 200X on a LEICA DML optical microscope with a video measurement system. This microscopy technique has provided reliable results which are statistically comparable to using a scanning electron microscope. Reproducibility of the measurements was also evaluated by comparing the measurement results from two different inspectors and using an ANOVA to analyze the significance of the factor. For misalignment analysis, a test was designed so to evaluate main effects such as fin thickness and allowance on the amount of misalignment. This evaluation was analyzed by a multifactor ANOVA (Type III Sums of Squares) under the condition that the p-value for a significant factor must be smaller than 0.05.

Before any experiments were run, a number of preliminary tests were conducted to calibrate the high temperature dimensions of the test fixture. The most important feature of the test fixture to be determined was the slot width at elevated temperature. A variety of test coupons with different width span were tested on the bonding fixture to identify where interference started relative to the expansion of both stainless steel and the graphite fixture.

Upon variation of fixture allowance, the laminae and fixture are either over-constrained or under-constrained. Buckling was found when the laminae were over-constrained. In this case, the width of laminae was longer than the slot size at the diffusion temperature. The mechanism of this fin buckling occurs when the force, due to the difference in CTE between the stainless steel laminae and the graphite fixture, exceeds the critical point of buckling and elastic limit. The magnitude of fin buckling at different amounts of interference can be calculated based on buckling theory. On the other hand, when the device was under-constrained, the width of laminae was shorter than the slot size at the bonding temperature, resulting in channel misalignment. The maximum misalignment was evaluated by looking at the actual clearance between fin width and slot size at the bonding temperature.

* Additional buckling calculation such as critical point vs. stiffness relation and the magnitude of fin buckling can be found in the full version of this article.

Figure 4 illustrates the magnitude of maximum deflection of warpage due to fin buckling with respect to the fixture allowance at the diffusion temperature from both theoretical prediction and experimental data. As can be seen from the graph, buckling begins for all three fin thickness at 10 μm of interference. The magnitude of warpage also increases as the interference increases. According to the ANOVA, it was concluded that there is no statistical evidence that the magnitude of warpage depends on the thickness of the shim under the scope of this experiment (p-value = 0.50). Furthermore, there was conclusive evidence that the mean warpage from the experimental data and the theoretical result were equal (t-stat = 1.42, df = 8). Its 95% confidence interval ranged from -0.01 to 0.05, which includes zero.

The error bars shown in Figure 4 are 95% confidence interval of the measured warpage. Each side of the interval is equal to $2 \cdot S_m$, where S_m is the standard error calculated from the variation of the warpage measurement. As can be seen from the graph, there are some variations of experimental results from the theory. Sources of error for this experiment might include the deviation of fin width from the patterning step either due to variation of beam diameter or the residual ejecta. Furthermore, the materials that were used in this experiment are thin shims, which might contain residual stress from a cold work processing that could play a key role in this variation.

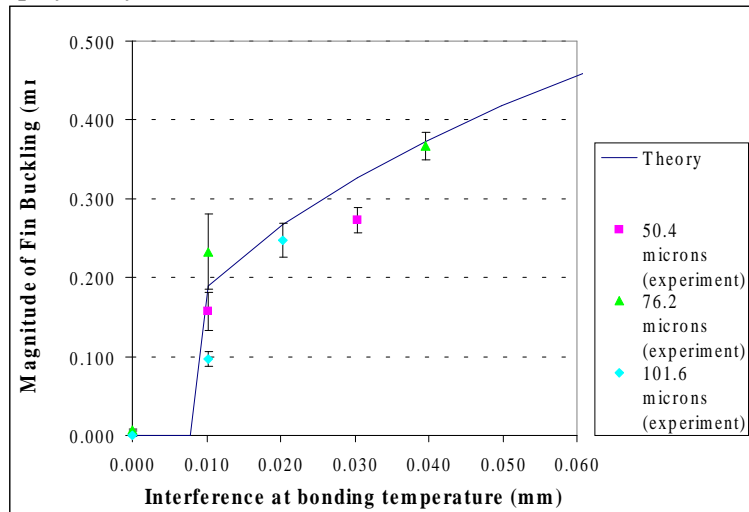


Figure 4. Magnitude of fin buckling versus the interference between fixture and laminae at bonding temperature with 95% confidence interval of standard deviation

Figure 5 displays the results for the misalignment analysis. Similar to Figure 4, this figure also presents the error bar based on the 95% confidence interval of the misalignment readings at 4 locations on the specimen. The test included the alignment analysis for both the under-constrained and over-constrained cases. With respect to this figure, precision alignment is achieved only in the area close to the exact constraint. As can be seen, the average and standard deviation for misalignment increases with clearance, and it also increases as the fin begins to buckle. Therefore, tight tolerance is required in order to attain a well-aligned channel. With respect to the ANOVA, the inspector factor was found to be not significant on misalignment (p-value = 0.9180) indicating a reproducible measurement technique. On the other hand, there is statistical evidence that misalignment depends on the allowance and measurement location (p-value < 0.05).

In conclusion, microlamination of metal structures for PI devices requires high temperature bonding. The TEER technique has been developed for precise alignment and bonding in the microlamination process. This research has been conducted to investigate the tolerance limits in a TEER bonding fixture for the purpose of minimizing the shape variation due to misregistration and fin buckling caused by excessive registration force during microlamination. Both analytical and experimental results are in good agreement within 95% confidence interval. Furthermore, it is evident that there are some

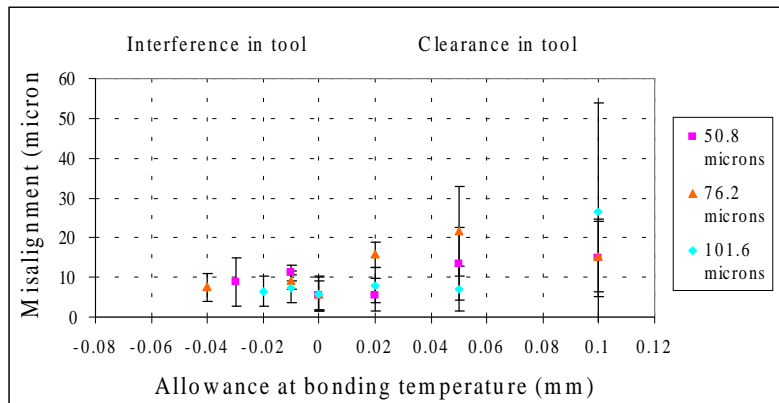


Figure 5. Misalignment vs. allowance between fixture and laminae at bonding temperature with 95% CI

tolerance limits in the TEER fixture that allows high-temperature microlamination to generate the multilayer structure with the minimal amount of shape variation. With respect to the nominal dimension specified in this study, the tolerance limit of 10 μm (interference) is where the fin starts to buckle, while the limit in misalignment is proportional to the clearance at the bonding temperature. The average channel-to-channel misalignment within this tolerance limit was about 6 μm . Finally, it was shown that the fixture tolerance has a finite fixed lower limit based on the elastic limit of the material. Therefore, as the thickness of laminae continues to decrease, the fixture tolerances will not need to continue to decrease below this lower limit.

- ¹ Martin, P. M., W. D. Bennett, and J. W. Johnson, "Microchannel Heat Exchangers for Advanced Climate Control," Proc. SPIE (v2639, 1996), pp82-88.
- ² Matson, D. W., P. M. Martin, W. D. Bennett, D. C. Stewart, and J. W. Johnson, "Laser Micromachined Microchannel Solvent Separator," Proc. SPIE, (v3223, 1997), pp253-259.
- ³ Matson, D. W., P. M. Martin, A. Y. Tonkovich and G. L. Roberts, "Fabrication of a Stainless Steel Microchannel Microcombustor Using a Lamination Process," Proc. SPIE (v3514, 1998), pp386-392.
- ⁴ Tonkovich, A. Y.; Zilka, J.L.; LaMont, M.J.; Wang, Y. and Wegeng, R.S. 1999. "Microchannel reactors for fuel processing applications," Chemical Engineering Science, 54(13): 2947-2951.
- ⁵ Paul, B. K., T. Dewey, D. Alman and R.D. Wilson, "Intermetallic Microlamination for High- Temperature Reactors," 4th Int. Conf. Microreaction Tech., Atlanta, GA, March 5-9, 2000, pp236-243.
- ⁶ Paul, B.K. and T. Terhaar, "Comparison of two passive microvalve designs for microlamination architectures," J Micromech. Microengr., (v10, 2000), pp15-20.
- ⁷ Esposito, A. 1988. Fluid Power with Applications. Prentice-Hall, 380-381.
- ⁸ NASA. 1988. National Space Transportation System Shuttle Reference Manual.
- ⁹ Haas, R.W., (1995), "Further Development of MMW and SMMW Platelet Feed Horn Arrays," ASP Conf. Ser., Vol. 75, pp. 99-105.
- ¹⁰ Haas, R.W., D. Brest, H. Mueggenburg, L. Lang, and D. Heimlich, (1993), Fabrication and Performance of MMW and SMMW Platelet Horn Arrays," Intl. J. Infrared and Millimeter Waves, 14(11), pp. 2289-2293.
- ¹¹ Young, M., (1997), "Platelet-Cooled Plasma Arc Torch," DOE Contract No. DE-AR21-93MC30361, Technology Development Data Sheet, (Morgantown, WV: Federal Energy Technology Center, 1997), 5-6.
- ¹² Anderson, J.J., 1989, U.S. Patent 4,875,619, Brazing of Ink Jet Print Head Components Using Thin Layers of Braze Material.
- ¹³ Unger, M.A., H. Chou, T. Thorsen, A. Scherer and S. Quake. 2000. Science, 288: pp 113-116.
- ¹⁴ Paul, B. K., Dewey, T., Alman, D., and Wilson, R. D., "Intermetallic Microlamination for High-Temperature Reactors," presented at 4th International Conference on Microreaction Technology, Atlanta, GA, 2000.
- ¹⁵ Ashley, S., "Turbines on a dime," *Mechanical engineering*, vol. 119, pp. 78-81, 1997.
- ¹⁶ Thomas, J. and B.K. Paul, "Thermally-Enhanced Edge Registration (TEER) for Aligning Metallic Microlaminated Devices," *Transactions of NAMRC XXX*, West Lafayette, IN, May 21-24, 2002, pp. 663-670.
- ¹⁷ Gere, J. M. and Timoshenko, S. P., *Mechanics of materials*. Boston: PWS-KENT Pub. Co., 1997.